MALEIMIDE BASED DONOR-ACCEPTOR FLUOROPHORE: MICROWAVE ASSISTED GREEN SYNTHESIS, PHOTOPHYSICAL AND DFT STUDY

Kirankumar S. Gosavi

Department of Chemistry, KVPS's Kisan Arts, Commerce and Science College, Parola,
Dist: Jalgaon, Maharashtra, India. Pin: 425111
Email-id: kirangosavi08@gmail.com
ORCID ID: 0000-0003-2143-0627

ABSTRACT
Report deals with green synthesis of 3-methoxy-1-methyl-4-phenyl-1H-pyrrole-2,5-dione derivatives, using microwave irradiation method to attribute its photophysical properties. The maleimide based donor-acceptor (D-A) fluorophore comprising of aryl substituent as donor and maleimide ring as acceptor unit. These fluorophore exhibited green and yellow emission colour with large Stokes shifts (> 125 nm) and fluorescence quantum yield ranging from 2% to 29%. The Density Functional Theory (DFT) simulations were performed in adjunct with the experimental study, to investigate the effect of electron donor and acceptor substituent on photophysical properties.

KEYWORDS
Donor-Acceptor, Maleimide; Fluorophore; DFT; HOMO-LUMO; Molecular Electrostatic Potentials

1. INTRODUCTION

The development of small organic fluorophores bearing electron donor-acceptor (D-A) type of architecture with distinctive photophysical and electrochemical properties is one of the most enthralling and exigent topic of the current interest[i]. The photophysical properties of the D-A systems are governed by the photoinduced intramolecular electron transfer from the donor unit to acceptor unit[ii]. Currently, efforts are focused on the modifying the nature of electron donating and accepting units of such D-A systems so as to tune desired photophysical properties, which could open up wide avenues for their diverse applications such as organic light emitting diodes (OLEDs)[iii], organic photovoltaics[iv], non-linear optical material[v], organic solar cells[vi], fluorescent probes[vii], bio imaging[viii], among others. Several elegant examples of D-A type of molecular systems based on oxazole[ix], triphenylamine[x], carbazol[xi], pyridine[xii] and Dibenzo[a, c]phenazine[xiii] etc. have been synthesized and utilized in variety of fluorescent applications.

Over last few years, maleimides (MIs) have been extensively studied owing to its spectacular fluorescent applications such as pH sensor[xiv], light emitting copolymers[xv], non-linear optical

(NLO) materials[xvi], metal ion sensor[xvii] and organic solar cells[xviii]. Recently, Patil and co-workers developed MI-carbazole based blue light emitting material and investigated its OLED application[xix]. Research group of Yasuda, studied 3,4-disubstituted MI based molecules for material applications[xx]. Gehlen and co-workers reported the synthesis and fluorescent study of D-A molecules based on MIs[xxi]. Nevertheless, fluorescent properties of the aryl-methoxy-maleimides are not much explored in the literature. In our previous work, we have reported the conventional synthesis and antimicrobial study the title MIs **3a-f** [xxii]. In this report, the alternative synthetic route by adopting microwave irradiation method is described for synthesis of the same MIs **3a-f** to study photophysical properties.

2. EXPERIMENTAL

2.1 REAGENTS AND CHEMICALS

All the reagents used in this study are of analytical grade produced from the commercial supplier S. D. Fine Chemicals private limited, Mumbai and were used without further purification. Spectroscopic grade solvents were used in the study.

2.2 EQUIPMENTS

IR spectra were recorded using Shimadzu FTIR-408 spectrophotometer as KBr pellets. UV-visible spectra were recorded using Schimadzu UV-106, UV-Vis spectra photometer. RF-5301 PC spectrofluorophotometer was used to record fluorescent spectra and all solvents used were of spectroscopic grade. ^{1}H and ^{13}C NMR spectra were recorded on Varian XL-300 spectrometer (300 MHz) in CDCl$_3$ and chemical shifts (δ) are reported in ppm with reference to TMS. Thermo Finnigan Eager 300 EA 1112 series analyser was used for elemental analyses.

2.3 GENERAL PROCEDURE FOR SYNTHESIS OF 3-METHOXY-1-METHYL-4-PHENYL-1H-PYRROLE-2,5-DIONE (3A-F)

A mixture of 3-methoxy-4-phenylfuran-2,5-dione **1a-c** (2.1 mmol) and methanamine **2a** / ethanamine **2b** (2.1 mmol) in anhydrous ethanol (5 mL) was refluxed in microwave oven at 100 W for 1 min. Progress of reaction was monitored by TLC. On completion, reaction mixture was concentrated in vaccuo. Solid was separated on aqueous work up, which was filtered and further purified by column chromatography using, hexane: ethyl acetate (8:2) as eluent. The physical and spectral data is summarized in table 3.

**Table 3.** Physical and Spectral Data of MIs **3a-f**

MI	Yield	MP (Lit.)^{xxii}	IR (cm^{-1})	NMR (300 MHz, CDCl$_3$, δ, ppm)
3a	95 %	78 °C (76-78 °C)	1758, 1712, 1612, 1133	^{1}H NMR: 2.90 (s, 3H), 4.16 (s, 3H), 7. 34- 7.75 (m, 5H); ^{13}C NMR: 23.46, 60.18, 113.17, 128.20, 128.65, 129.05, 130.39, 166.18, 170.73, 171.39
3b	93 %	74 °C (74-76 °C)	1764, 1712, 1610, 1122	^{1}H NMR: 1.24 (t, 3H, J = 7.2 Hz), 3.60 (q, 2H, J = 7.2 Hz), 4.23 (s, 3H), 7.33-7.90 (m, 5H)
3c	96 %	102 °C (102-104 °C)	1756, 1705, 1633, 1114	^{1}H NMR: 3.05 (s, 3H), 4.32 (s, 3H), 7.45 (d, 2H, J = 8.4 Hz), 7. 86 (d, 2H, J = 8.4 Hz); ^{13}C NMR: 23.39, 60.40, 111.92, 127.00, 128.48, 130.02, 134.38, 151.67, 165.80, 169.78
3d	92 %	50 °C (48-50 °C)	1755, 1702, 1621, 1107	^{1}H NMR: 1.28 (t, 3H, J = 7.5 Hz), 3.65 (q, 2H, J = 7.5 Hz), 4.25 (s, 3H), 7.42 (d, 2H, J = 8 Hz), 7.81 (d, 2H, J = 8 Hz)
3e	90 %	56 °C (56-58 °C)	1764, 1713, 1607	^{1}H NMR: 3.03 (s, 3H), 3.85 (s, 3H), 4.24 (s, 3H), 6.92 (d, 2H, J = 8.8 Hz), 7.84 (d, 2H, J = 8.8 Hz)

| 3f | 95 % | 60 °C (58-60 °C) | 1749, 1698, 1633, 1136 | ^{1}H NMR: 1.10 (t, 3H, *J* = 7.2 Hz), 3.44 (q, 2H, *J* = 7.2 Hz), 3.78 (s, 3H), 4.17 (s, 3H), 7.02 (d, 2H, *J* = 8.8 Hz), 7.77 (d, 2H, *J* = 8.8 Hz) |

3. RESULTS AND DISCUSSION
3.1 SYNTHESIS
In literature, there are several reports for the synthesis of MIs from corresponding maleic anhydrides[xxiii,xxiv]; however it involves time consuming procedures with carcinogenic solvents and non-green reagents. Obviously any improvised greener approach towards the synthesis of such compounds would be greatly appreciated. Our group is mainly focusing on the synthesis of MIs to study its material and biological applications[xxv-xxviii]. In our previous manuscript[xxii], we have reported the synthesis of the MIs **3a-f** by conventional method. Taking aforementioned facts into an account, herein the microwave assisted greener route for synthesis of MIs **3a-f** is described (Scheme 1). The target compounds 3-aryl-4-methoxy *N*-alkyl MIs **3a-f** were prepared by reacting corresponding maleic anhydride derivatives **1a-c** with methyl amine **(2a)** / ethyl amine **(2b)** in ethanol at reflux condition under microwave irradiation for 1 minute with excellent yields. The structures of all the MIs were authenticated by IR, NMR, and elemental analysis.
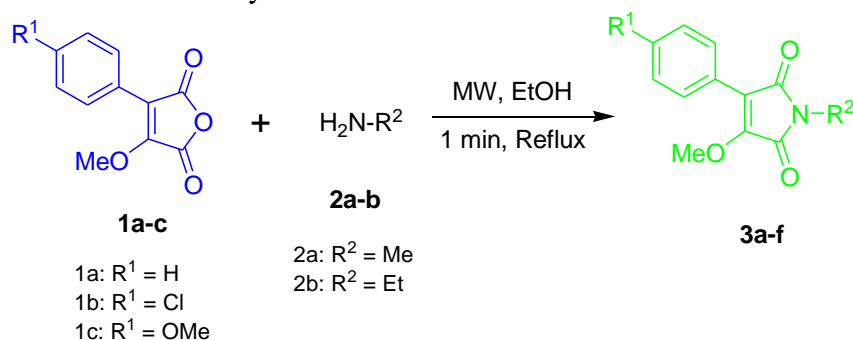
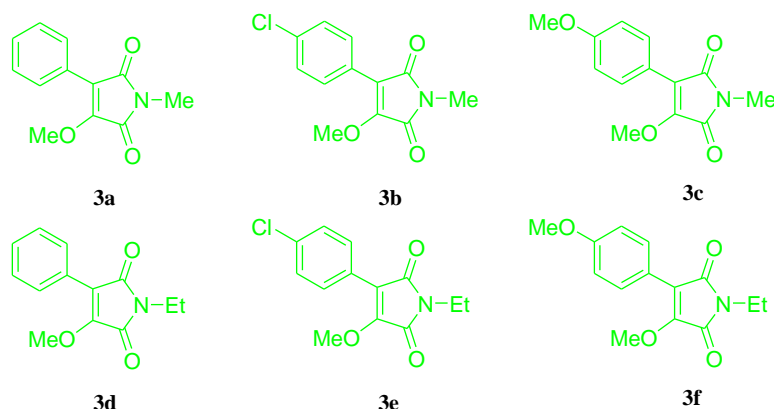**Scheme 1.** Microwave assisted synthesis of MIs **3a-f**

Figure 1. Chemical structures of synthesized MI **3a-f**

3.2 PHOTOPHYSICAL STUDY
The photophysical properties of fluorophore **3a-f** were studied by UV-visible absorption and fluorescence measurements in chloroform solution at 2 x 10^{-5} M concentration. Their electronic absorption, fluorescence, Stoke's shift and fluorescence quantum yields data are illustrated in table 1 and figure 2. Excitation of synthesized fluorophores exhibited green fluorescence colour. The maleimide based donor-acceptor (D-A) fluorophore **3a-f** are comprised of aryl substituent as donor and maleimide ring as acceptor unit. One of the prime objectives of studying the photophysical behaviour of these compounds was to investigate the

effect of varying donor units. The MIs **3a-f** displayed broad absorption maxima (λ_{abs}) in the range of 373 nm to 398 nm which can be attributed to the intramolecular charge transfer (ICT) arising as an outcome of electron transfer from aryl donor to MI acceptor.

The emission maxima (λ_{em}) for *N*-methyl MI **3a-c** were observed at around 499 nm, 500 nm and 525 nm respectively. The electron donating strength of aryl substituent intensifies from **3a** to **3c**, this results in red shifted emission maxima in the order of **3c** > **3b** > **3a** which was observed due to donor-acceptor type of electronic effect with ICT[xxi]. Similar type of red shift was observed for *N*-ethyl MI **3d-f**. Furthermore, the effect of *N*-alkyl substituent on optical properties of MI was investigated, the absorption and emission maxima of *N*-ethyl MI **3d-f** showed red shift of 1-5 nm than corresponding *N*-methyl MI **3a-c**.

The minimum overlap in the absorption and emission spectra of the compounds, accounts for the large Stokes shift values. Fluorophores **3a-f** exhibited Stokes shift values in the range of 125 nm to 130 nm, ascribed to solvent stabilization of fluorophore in its excited state[xxi]. The higher value of Stokes shift for **3c** and **3f** than rest of compounds indicated the effect of substituent on the value of Stokes shift is measure of the strong electron D-A type of interaction.

Table 1. Observed photophysical properties of MIs **3a-f** in CHCl$_3$ at room temperature

Fluorophore	[a]λ_{abs} (nm)	[b]λ_{em} (nm)	[c]$\Delta\lambda$ (nm)	[d]Φ_f (%)
3a	373	499	126	02
3b	375	500	125	29
3c	396	525	129	05
3d	374	501	127	18
3e	378	505	127	12
3f	398	528	130	10

[a] Absorption maxima, [b] Emission maxima, [c] Stokes Shift, [d] Fluorescence quantum yield (%).

The fluorescence quantum yield was calculated by comparative method using anthracene (Φ: 0.27) as a reference[xxix,xxx]. From Table 1 it was clear that compound **3b** showed highest fluorescence quantum yield of 29% that could be attributed to enhanced fluorescence intensity.
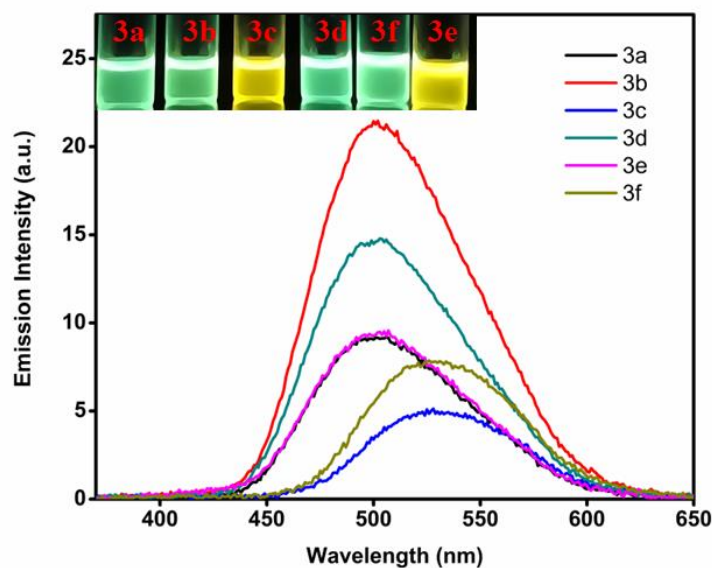

Figure 2. Emission graphs of MIs in CHCl$_3$

3.3 COMPUTATIONAL STUDY
3.3.1 OPTIMIZED STRUCTURE
Density Functional Theory (DFT) calculations were performed on Gaussian 09W software. The optimized structures of fluorophores were obtained using DFT/B3LYP method with a basis set of 6-31G (d, p)[xxxi]. The optimized structure of MI **3b** is given in figure 3.
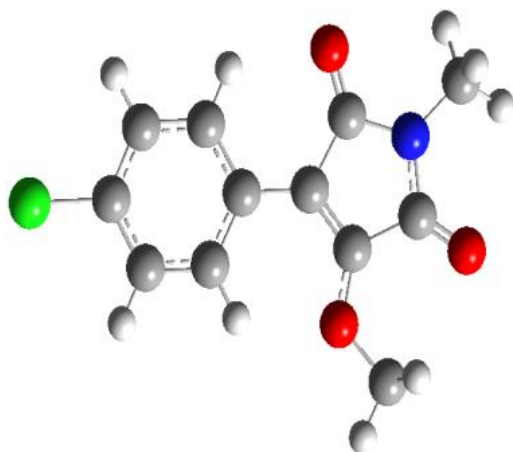

Figure 3. Optimized diagrams of MIs **3b** using DFT/B3LYP method

3.3.2 FRONTIER MOLECULAR ORBITAL ANALYSIS
The energies and allocations of frontier molecular orbitals are the very important descriptors in the computational chemistry. The chemical reactivity, active site and stability of the molecule can be predicted with the help of Highest Occupied Molecular Orbital (HOMO) and Lowest Unoccupied Molecular Orbital (LUMO). The HOMO and LUMO represents the electron donating and withdrawing ability of the molecule respectively. Energy gap between these frontier molecular orbitals play vital role as analytical parameter in determining and understanding change transfer behaviour of the molecules.

Table 2. DFT calculations of compounds **3a-f** in eV

Compound	$^a E_{HOMO}$	$^b E_{LUMO}$	$^c \Delta E_g$	$^d \eta$	$^e S$
3a	- 5.896	- 2.353	3.54	1.771	0.564
3b	- 6.007	- 2.525	3.48	1.741	0.574
3c	- 5.447	- 2.220	3.22	1.613	0.620
3d	- 5.888	- 2.331	3.56	1.778	0.562
3e	- 5.994	- 2.506	3.49	1.744	0.573
3f	- 5.436	- 2.206	3.23	1.615	0.619

^{a} Energy of HOMO, ^{b} Energy of LUMO, ^{c} HOMO-LUMO energy gap, ^{d} chemical hardness, ^{e} chemical softness

The calculated energy of HOMO (E_{HOMO}), LUMO (E_{LUMO}) and related properties calculated by DFT are summarized in Table 2. The E_{HOMO} of all compounds were in the range of - 5.436 to - 6.007 eV, while E_{LUMO} were in the range of - 2.206 to - 2.525 eV. Due to introduction of electron donating methoxy substituent in compound **3c** and **3f**, E_{HOMO} and E_{LUMO} values gets decreased and resulted in low HOMO-LUMO energy gap value (ΔE_g) of 3.22 and 3.23 eV respectively which leads to significant red shift. The ground state optimised structure and 3D surface plot of HOMO and LUMO for compound **3a-f** are given in the figure 4. It was observed that HOMO located over the aromatic ring while LUMO was located over the MI ring.

Chemical hardness (η) is a qualitative identification of polarizability of molecule. The hard molecule have large HOMO-LUMO energy gap value, due to this they are stable while soft molecules have small energy gap value and require small extent of energy for excitation and

hence soft molecules are more reactive[xxxii]. From energies of HOMO and LUMO, chemical hardness of the molecule can determine by formula[xxxiii].

$\eta = E_{LUMO} - E_{HOMO} / 2$

Chemical softness (S) is the inverse of chemical hardness[xxxiii] i.e. $S = 1 / \eta$.

From Table 2, it was observed that the value of chemical hardness (η) is highest for compound **3d** (1.778 eV) while the value of chemical softness (S) is highest for compound **3c** (0.620 eV). This indicates that compound **3d** is most stable and compound **3c** is most reactive amongst the studies MI **3a-f**.
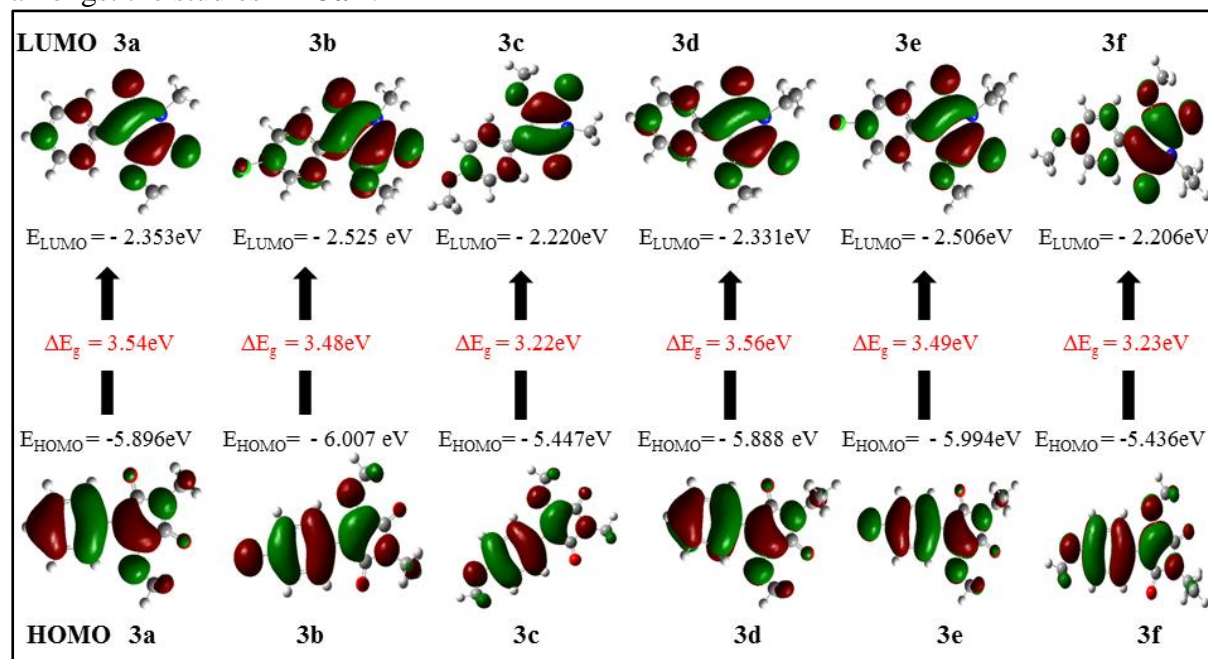

Figure 4. Ground state optimised structure and 3D surface plot of HOMO and LUMO for MIs **3a-f**

3.3.3 MOLECULAR ELECTROSTATIC POTENTIALS (MEP)

The molecular electrostatic potential (MEP) map guides to identify the probable sites for the nucleophilic and electrophilic attack and hydrogen bonding interactions in the molecules. The coloured region in the MEP signifies these reactive sites for the nucleophilic and electrophilic attack. In MEP, colour grading is used to identify the region of the positive and negative electrostatic potential in the molecule[xxxiii]. The MEP map of compounds **3a-f** are given in figure 5, in which the blue colour (i.e. positive electrostatic potential) around methyl group represents the nucleophilic site while red colour (i.e. negative electrostatic potential) around the carbonyl group represents the electrophilic site.

3a　　　　　**3b**　　　　　**3c**
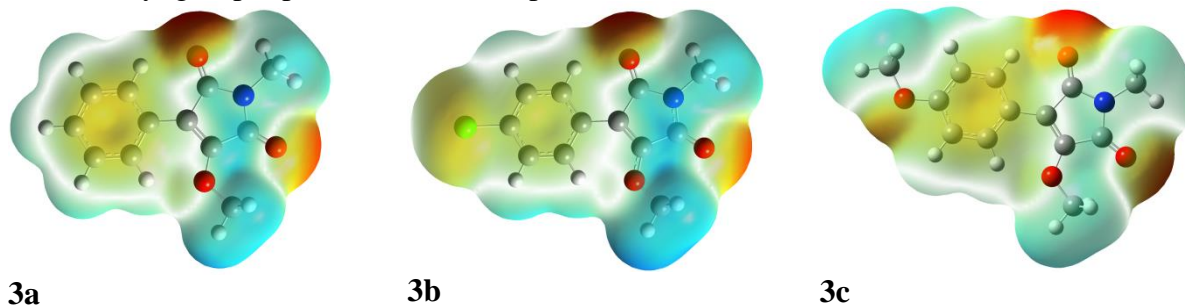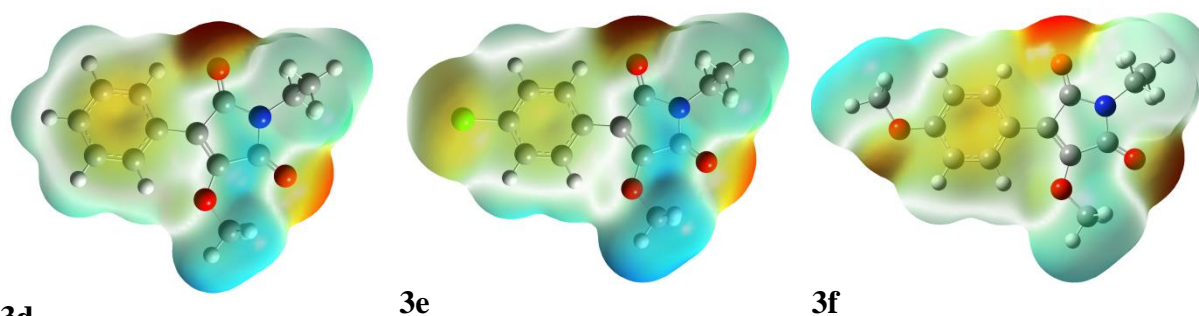
3d   **3e**   **3f**

Figure 5. Molecular electrostatic potential maps for MIs **3a-f**

4. CONCLUSION

In conclusion, six fluorophores with D-A framework comprising of aryl substituent as donor and maleimide ring as acceptor has been synthesized using microwave assisted green protocol. The emitting behaviour of the MIs is dependent upon the donating capacity of donor (aryl substituent). The electron donating 4-methoxyphenyl substituted MI **3f** showed red shift in the emission maxima (λ em = 528 nm) than its corresponding phenyl substituted maleimide **3d** (λ em = 501 nm). From DFT calculations, the E_{HOMO}, E_{LUMO}, ΔE_g, chemical hardness (η) and chemical softness (S) were estimated and it was concluded that compound **3d** is comparatively more stable and compound **3c** is comparatively more reactive amongst investigated MIs **3a-f**.

5. ACKNOWLEDGMENTS

6. REFERENCES

i.   Carbas B.B.; Noori H.A.; Kavak E.; Kaya Y.; Kıvrak A.; Optical, electrochemical and DFT studies of donor-acceptor typed indole derivatives; Journal of Molecular Structure; 2023, **1271**, 134129.

ii.   Garain S.; Ansari S.N.; Kongasseri A.; Garain B.C.; Pati S.K.; and George S.J.; Room temperature charge-transfer phosphorescence from organic donor–acceptor Co-crystals; Chem. Sci.; 2022, **13**, 10011.

iii.   Zhou X.; Yang H.; Chen Z.; Gong S.; Lu Z.H.; Yang C.; Naphthyridine-based emitters simultaneously exhibiting thermally activated delayed fluorescence and aggregation-induced emission for highly efficient non-doped fluorescent OLEDs; J. Mater. Chem. C; 2019, **7**, 6607.

iv.   Wan X.; Li C.; Zhang M.; Chen Y.; Acceptor-donor-acceptor type molecules for high performance organic photovoltaics-chemistry and mechanism; Chem. Soc. Rev.; 2020, **49**, 2828.

v.   He Q.; Shahid M.; Panidi J.; Marsh A.V.; Huang W.; Daboczi M.; Kim J.; Fei Z.; Anthopoulos T.D.; Heeney M.; A versatile star-shaped organic semiconductor based on benzodithiophene and diketopyrrolopyrrole; J. Mater. Chem. C; 2019, **7**, 6622.

vi.   Torrientes R.S.; Gavrik A.; Isakova A.; Abudulimu A.; Calbo J.; Arago J.; Santos J.; Orti E.; Martin N.; Dyakonov V.; Luer L.; Minimizing geminate recombination

losses in small-molecule-based organic solar cells; J. Mater. Chem. C; 2019, **7**, 6641.

vii.   Elana M.S.; Ciubaa M.A.; Levitus M.; Photophysical processes in single molecule organic fluorescent probes; Chem. Soc. Rev.; 2014, **43**, 1057.

viii.   Joanna L; Daniel D.; Stiegert O.; Jose M.; Beloqui M.; Rizzello L.; Battaglia G.; Clarke TM.; Howorka S.; Wilden J.D.; Exploring the Relationship between BODIPY Structure and Spectroscopic Properties to Design Fluorophores for Bioimaging, Chemistry- A European journal; 2020, **16**, 863.

ix.   Liu B.; Chen L.; Wang X.; Lic L.; Wang G.; Nonylbisoxazole-based donor-acceptor copolymers for polymer solar cells; New J. Chem.; 2021, **45**, 2710.

x.   Yadav I.S.; Alsaleh A.Z.; Misra R.; D'Souza F.; Charge stabilization via electron exchange: excited charge separation in symmetric, central triphenylamine derived, dimethylaminophenyl–tetracyanobutadiene donor–acceptor conjugates; Chem. Sci.; 2021, **12**, 1109.

xi.   Ebeling R. Arasu N.; Bensch L.; Lammers B.; Mayer B.; Müller T.; Vázquez J.; Karthäuser S.; Preservation of the donor–acceptor character of a carbazole–phenalenone dyad upon adsorption on Pt.; Nanoscale Adv.; 2021, **3**, 538-549.

xii.   Nagarasu P.; Kundu A.; Pitchaimani J.; Anthony S.P.; Moon D.; Madhu V.; Structure controlled solvatochromism and halochromic fluorescence switching of 2,2′-bipyridine based donor–acceptor derivatives; New J. Chem.; 2020, **44**, 14421.

xiii.   Boxi S.; Jana D.; Parui P.; Ghorai B.K.; Dibenzo[a, c]phenazine-Based Donor-Acceptor (D–A) Tetra Branched Molecules: Fine Tuning of Optical Properties; Chemistry Select; 2018, **3**, 6953.

xiv.   Kato T.; Naka K.; Arylaminomaleimides as a New Class of Aggregation-induced Emission-active Molecules Obtained from Organoarsenic Compounds.; Chem. Lett.; 2012, **41**, 1445.

xv.   Chan L.H.; Lee U.D.; Chen C.T; Achieving saturated red photoluminescence and electroluminescence with readily synthesized maleimide-arylamine copolymers; Tetrahedron; 2006, **62**, 9541.

xvi.   Jeng R.J.; Chang C.C.; Chen C.; Chen C.T; Su W.; Thermally stable crosslinked NLO materials based on maleimides; Polymer; 2003, **44**, 143.

xvii.   Kaletas B.K.; Williams R.M.; Konig B.B; Cola L; Strong fluorescence enhancement of 2-bromo-3-(1H-indol-3-yl)maleimide upon coordination to a Lewis-acidic metal complex; Chem. Commun.; 2002, 776.

xviii.   He X.; Yin L.; Li Y.; Efficient design and structural modifications for tuning the photoelectric properties of small-molecule acceptors in organic solar cells; New J. Chem.; 2019, **43**, 6577.

xix.   Venkatramaiah N; Kumar G.D.; Chandrasekaran Y. Ganduri R.; Patil S.; Efficient Blue and Yellow Organic Light-Emitting Diodes Enabled by Aggregation-Induced Emission; ACS Appl. Mater. Interfaces; 2018, **10**, 3838.

xx.   Jang M.E.; Yasuda T.; Lee J.; Lee S.Y.; Adachi C.; Organic Light-Emitting Diodes Based on Donor-Substituted Phthalimide and Maleimide Fluorophores; Chem. Letts; 2015, **44**, 1248.

xxi.   Lauer M.H.; Drekener R.L.; Correia C.D.; Gehlen M.H.; Fluorescence from bisaryl-substituted maleimide derivatives; 2014, **13**, 859.

xxii.   Gosavi K.S.; Mahale K.A.; Patil N.S.; Patil S.V.; Synthesis and biological evaluation of novel 3-aryl-4-methoxy N-alkyl maleimides; Indian Journal of Chemistry; 2021, **60B**, 473.

xxiii.   Sortino M.; Garibotto F.; Filho V.C.; Gupta M.; Enriz R.; Zacchino S.; Antifungal,

cytotoxic and SAR studies of a series of *N*-alkyl, *N*-aryl and *N*-alkylphenyl-1,4-pyrrolediones and related compounds; Bioorganic & Medicinal Chemistry; 2011,**19**, 2823

xxiv.   Matuszak N.; Muccioli G.G.; Labar G.; Lambert D.M.; Synthesis and in Vitro Evaluation of N-Substituted Maleimide Derivatives as Selective Monoglyceride Lipase Inhibitors; J. Med. Chem, 2009, **52**, 7410.

xxv.   Gosavi K.S.; Mahale K.A.; Patil S.V.; Synthesis and Photophysical Study of [60]Fullerene-Maleimide Dyads; J. Fluoresc.; 2020, **30**, 223.

xxvi.   Patil S.V.; Mahale K.A. Gosavi K.S.; Deshmukh G.B.; Patil N.S.; Solvent-mediated One-pot Synthesis of Cyclic N-Substituted Imides; Organic Preparations and Procedures International; 2013, **45**, 314.

xxvii. Gosavi K.S.; Mahale K.A.; Patil N.S.; Patil S.V.; Synthesis of Novel 3-Methoxy-4-Phenyl-1-p-Tolyl-1H-Pyrrole-2,5-Dione Derivatives and Study of Their Antimicrobial Activity; Chemistry & Biology Interface; 2019, **9**, 266.

xviii. Gosavi K.S.; Exploration of [60]fullerene-maleimide derivatives as antimicrobial agents, Heterocyclic Letters; 2020, **10**, 435.

xxix.   Williams A.R.; Winfield S.; Miller J.N.; Relative fluorescence quantum yields sing a computer controlled luminescence spectrometer; Analyst; 1983, **108**, 1067.

xxx.   Patil V.S.; Padalkar V.S.; Sekar N.; 2-Methyl-4-oxo-N-(4-oxo-2-phenyl substituted-1,3-thiazolidin-3-yl)-3,4-dihydroquinazoline-5-carboxamides-A   New Range of Fluorescent Whiteners: Synthesis and Photophysical Characterization; J. Fluoresc.; 2014, **24**, 1077.

xxxi.   Frisch M.J.; Trucks G.W.; Schlegel H.B.; Scuseria G.; Robb M.A.; Cheeseman J.R.; Scalmani G.; Barone V.; Gaussian-09; 2010; Revision B.01, Gaussian, Inc. Wallingford CT.

xxxii. Muthu S.; Prasath M.; Paulraj E.I.; Balaji R.A.; FT-IR, FT-Raman spectra and ab initio HF and DFT calculations of 7-chloro-5-(2-chlorophenyl)-3-hydroxy-2,3-dihydro-1H-1,4-benzodiazepin-2-one; Spectrochim. Acta Part A Mol. Biomol. Spectrosc.; 2014, **120**, 185.

xxiii. Akbari Z.; Stagno C.; Iraci N.; Efferth T.; Omer E.A.; Piperno A.; Montazerozohori M.; Feizi-Dehnayebi M.; Micale N.; Biological evaluation, DFT, MEP, HOMO-LUMO analysis and ensemble docking studies of Zn(II) complexes of bidentate and tetradentate Schiff base ligands as antileukemia agents; Journal of Molecular Structure; 2024, **1301**, 137400.

Received on December 28, 2023.